Chapter 8

Electrical Characterization of Thin-Film Transistors Based on Solution-Processed Metal Oxides

João P. Braga, Guilherme R. De Lima, Giovani Gozzi and Lucas Fugikawa Santos

Additional information is available at the end of the chapter

http://dx.doi.org/10.5772/intechopen.78221

Abstract

This chapter provides a brief introduction to thin-film transistors (TFTs) based on transparent semiconducting metal oxides (SMOs) with a focus on solution-processed devices. The electrical properties of TFTs comprising different active layer compositions (zinc oxide, aluminum-doped zinc oxide and indium-zinc oxide) produced by spin-coating and spray-pyrolysis deposition are presented and compared. The electrical performance of TFTs is evaluated from parameters as the saturation mobility (μ_{sat}), the TFT threshold voltage (V_{th}) and the on/off current (I_{on}/I_{off}) ratio to demonstrate the dependence on the composition of the device-active layer and on ambient characterization conditions (exposure to UV radiation and to air).

Keywords: semiconducting metal oxides, electrical properties, thin-film transistors, spray-pyrolysis, spin-coating

1. Introduction

The development of electronic and optoelectronic devices attending the increasing demand of new features like high-resolution, fast response, transparency and flexibility has motivated the pursuit of circuits using new active materials and/or new processing technologies. In this sense, semiconducting metal oxides (SMOs) as zinc oxide (ZnO) [1–9] and related compounds like aluminum-doped zinc oxide (AZO) [10–13], indium zinc oxide (IZO) [14, 15] and indium gallium zinc oxide (IGZO) [16, 17] are promising materials for flexible, transparent and high-performance electronics.

SMOs are particularly interesting to be used as the active layer of thin-film transistors (TFTs), which constitute the basic electronic device for drive circuits of active-matrix displays (AMDs)

and more sophisticated logic circuits which can be used in memories, microcontrollers and processors. Recently, the manufacture of metal oxide thin films using organic precursor solutions or nanoparticle suspensions became widespread [1–10], permitting the use of low-cost and nonsophisticated deposition techniques as spin coating, ink-jet printing and spray pyrolysis [18–21]. These techniques produce very uniform and homogeneous nanoscaled films, with high control of thickness and of other physical properties. This chapter aims to describe briefly the manufacturing processes of TFTs using solution-processed metal oxides as the semiconducting active layer, focusing on the electrical characterization and the study of the electrical properties relevant to the evaluation of device performance.

2. Semiconducting metal oxide thin-film transistors

Semiconducting metal oxides are promising materials to replace semiconductors as amorphous silicon (a-Si) and polycrystalline silicon (poly-Si) in applications as drive circuits of active-matrix (AM) flat-panel displays commonly used in cell phones, notebooks and monitor screens. They present interesting features like high optical transmittance in the visible range, high electronic mobility, low fabrication cost and compatibility to large-area applications. In the past 15 years, substantial efforts have been made to achieve high-performance SMO TFTs which are suitable to transparent and flexible substrates, enabling the development of the next generation of thin-flat panel displays.

As the active layer of thin-film transistors, SMOs usually present field-effect mobilities higher than 10 $cm^2.V^{-1}.s^{-1}$ (with a reported values as high as 172 $cm^2V^{-1}s^{-1}$) when deposited by techniques like RF sputtering and pulsed-laser deposition [22–27], which is a great advantage if we consider that a-Si can hardly present field-effect mobilities higher than 1 $cm^2V^{-1}s^{-1}$. Compared to poly-Si, which presents carrier mobilities up to 100 $cm^2V^{-1}s^{-1}$, SMOs present higher-film uniformity and considerably lower-processing temperatures, allowing large-area applications and low-production costs.

2.1. Zinc oxide and related compounds

Zinc oxide and related compounds and alloys are the most studied semiconducting metal oxides used as active materials in electronic and optoelectronic devices. Applications in thin-film transistors, light-emitting diodes and UV photodetectors and photosensors are feasible due to their chemical stability and exceptional electronic and physical properties. ZnO is transparent in the whole visible spectrum, has a wide (direct) band gap (E_g ~ 3.37 eV), a high electron mobility and large exciton binding energy (~ 60 meV). It crystallizes in either cubic zinc blend or hexagonal wurtzite structure, with the latter being the most thermodynamically stable form at ambient conditions. At relatively high temperatures and pressures, the rocksalt (NaCl) crystalline structure can also be formed. **Figure 1** shows the representation of the ZnO unit cell with wurtzite structure. In this structure, each cation is surrounded by four anions at the corners of a tetrahedron and vice versa, with a typically sp^3 covalent bonding nature coordination.

Even though large single crystals of ZnO can be obtained using appropriate substrates via very controlled deposition techniques like pulsed laser deposition (PLD), chemical vapor deposition

http://dx.doi.org/10.5772/intechopen.78221

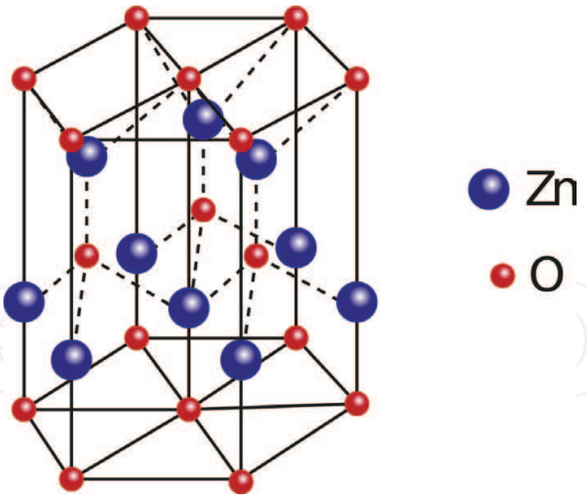

Figure 1. Representation of the ZnO unit cell with wurtzite structure.

(CVD) and molecular-beam epitaxy (MBE), most of the technological applications use thin films which are polycrystalline or formed by large-size crystallites separated by grain boundaries (as obtained by RF sputtering), presenting limitations to the charge-carrier transport.

Zinc oxide is known as an unintentionally doped semiconductor, due to the presence of native (intrinsic) defects in the crystal lattice. These defects can be vacancies (missing atoms at regular lattice positions), interstitials (extra atoms occupying interstices in the lattice) and antisites (an anion occupying a cation position in the lattice or vice versa) [28]. Although controversial, oxygen vacancies and zinc interstitials have been often credited as the major source of the observed unintentional n-type conductivity in ZnO [9, 24, 29–32]. The oxygen vacancies (V_o) have the lowest formation energy among the native defects which act as donors in ZnO and are frequently associated in the literature to the n-type character of ZnO. However, density functional calculations have shown that V_o's behave more as deep donor defects instead of shallow donors and some authors affirm that they cannot be responsible for the n-type carrier transport in ZnO [33, 34]. Zinc interstitials (Zn_i), on the other hand, behave as shallow donors but are usually present in very low concentrations in n-type ZnO. An alternative explanation is that n-type conductivity is due to unintentional substitutional hydrogen impurities, which is supported by theoretical calculations [35, 36]. Therefore, the actual origin of n-type conductivity in ZnO still remains controversial since a great number of experimental reports on the electrical properties of thin-film ZnO electronic devices demonstrate a correlation between oxygen concentration (during deposition and/or device handling) and the electrical conductivity [23, 37, 38], disagreeing with results obtained from first-principle theoretical calculations in crystals.

2.1.1. Thin-film deposition methods

Electronic and optoelectronic devices based on metal oxides usually comprise thin-films deposited on appropriate substrates. High-quality crystalline ZnO layers can be obtained by using extremely controlled deposition processes like pulsed laser deposition (PLD), molecular beam epitaxy (MBE), chemical vapor deposition (CVD), metal–organic chemical vapor deposition (MOCVD) and atomic layer deposition (ALD) [12, 33, 39] and even using less sophisticated methods like RF magnetron sputtering [22–25].

However, with the recent increase on field-effect mobility of TFTs produced with the active layer deposited from solution processes [3, 5, 6, 17, 19, 20], more attention has been attracted to the possibility of using very simple and low-cost deposition methods to obtain high-performance TFTs. Solution-based deposition processes allow the use of techniques like dip coating, spin coating, spray coating, ink-jet printing, silk screen and numerous others which are compatible to large-area, flexible, affordable and scalable applications. **Figure 2** shows a schematic representation of the basic features of common low-cost deposition methods for fabrication of metal oxide TFTs. RF magnetron sputtering (**Figure 2a**) and PLD (**Figure 2b**) produce highly crystalline films with relatively good thickness and uniformity control; however, target materials, vacuum and partial gas pressure systems as well as RF source or laser beam are needed, making these techniques more sophisticated when compared to solution-based processes like spin coating (**Figure 2c**), airbrush spray pyrolysis (**Figure 2d**) or ultrasonic spray pyrolysis (**Figure 2e**).

Spin coating is a widespread used deposition technique which yields very thin (ranging from few nanometers up to micrometers) and uniform films by spreading a solution of the desired material onto cleaned substrates and making them spin at high rotation speeds (about 1000–8000 rpm) promoting solvent evaporation. The technique is very successful in the formation of organic or polymeric films but can be used to deposit inorganic materials solutions or suspensions as well. Spray pyrolysis is based on spraying a solution of an organic precursor onto a preheated substrate (usually at a temperature above the degradation temperature of the

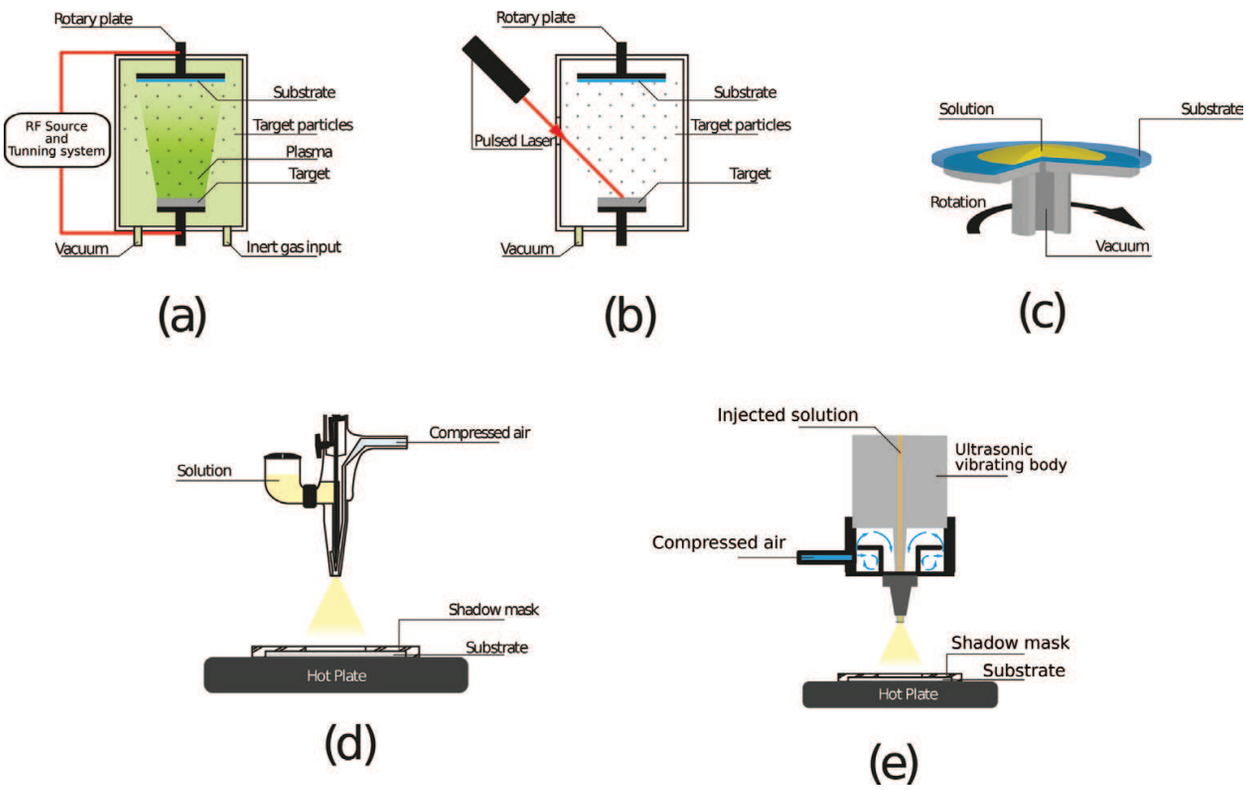

Figure 2. Summary of the frequently used low-cost deposition techniques used to produce electronic devices based on semiconducting metal oxides. (a) RF magnetron sputtering; (b) pulsed laser deposition (PLD); (c) spin-coating; (d) airbrush spray-pyrolysis (ASP); and (e) ultrasonic spray-pyrolysis (USP).

organic phase of the precursor material) to produce thin and highly uniform metal-oxide films. Difference between airbrush and ultrasonic spray deposition is that, in the former, a mechanically actuated needle is responsible to release the precursor solution, which flows due to gravity through the spray nozzle whereas in the latter, a piezoelectric nozzle driven by an ultrasonic power supply is used to nebulize the precursor solution which is injected by a micro-syringe pump. In both cases, compressed dry air or inert gas is used to carry the nebulized material. Ultrasonic spray has the advantage to provide higher droplet size control (in the order of tens of microns) and to economize precursor solution whereas airbrush is a low-cost and simple alternative to obtain very uniform films which can be used to produce high-performance TFTs [13].

2.2. Solution-processed metal oxide thin films

Solution-processed metal oxide thin films used as the active layer of transistors can be deposited from any of the techniques mentioned previously. An important key to obtain high performance and reproducible devices is the film uniformity, which can be macroscopically inspected by visual observation (translucent and shiny films usually represent superior quality films) or microscopically from techniques like profilometry (which can measure the surface roughness), atomic force microscopy (AFM) or scanning electron microscopy (SEM). The solution preparation method plays a significant role in the film formation and must be meticulously planned to obtain improved performance devices. The most commonly used solution processing techniques used to produce SMO TFTs are based on: (i) the calcination or pyrolysis of an organic precursor of the desired metal oxide which is soluble in an organic solvent or (ii) on the physical agglomeration or chemical reaction of previously synthesized nanoparticles which can form a uniform suspension in water or in other polar protic solvents.

2.2.1. Organic precursor pyrolysis

The solutions used to prepare SMO films deposited by spin-coating and spray technique are frequently obtained by the dissolution of organic salts containing the metallic atom which forms the metal oxide. **Figure 3** shows the scheme that most common organic salts used metal oxide precursors. Special attention is devoted to zinc acetate dihydrate (**Figure 3a**), which is the basic compound used to obtain ZnO and is soluble in water and other polar protic solvents like ethanol, isopropanol and methanol. Very often, 2-methoxyethanol is used as the solvent with ethanolamine as stabilizer [11, 15, 26] due to the credited better precursor dissolution and film formation.

Spin-coating deposition is commonly carried out using solution concentrations in the (0.03–0.3 M) range to originate organic precursor films which undergo a pyrolysis process by heating up the substrates in a hotplate or in an oven at temperatures above the degradation temperature of the organic compound (usually above 300°C). After the thermal decomposition of the precursor organic phase, oxide agglomerates intermediated by voids, but which can be interconnected along macroscopic distances (superior to few millimeters), are formed. To form a continuous and uniform oxide film, the multiple deposition of precursor layers by spin coating is performed, intercalated by the thermal treatment process to promote the oxide formation and to avoid the dissolution of the previous layers [14].

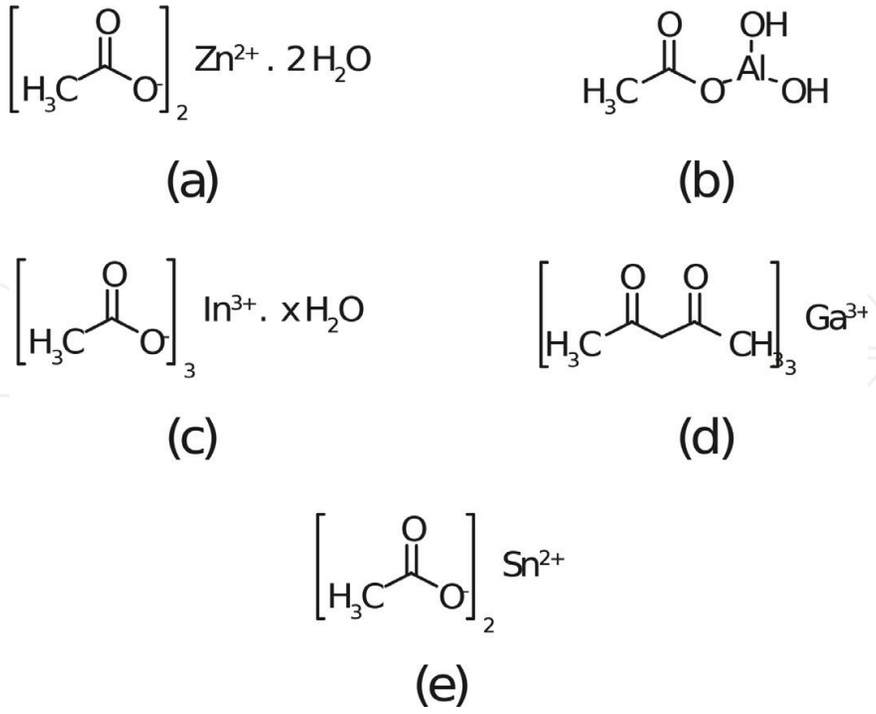

Figure 3. Scheme of the chemical structure of most commonly used organic precursors of metal oxides. (a) Zinc acetate dihydrate; (b) aluminum acetate dibasic; (c) indium acetate hydrate; (d) galium acetyl acetonate; (e) tin acetate.

Spray-pyrolysis deposition, on the other hand, is a much simpler method which does not require intermediate processing like the multilayer spin-coating method described earlier, being more suitable to industrial scalable processes. During spray deposition, precursor solution droplets reach a substrate heated up to a temperature much higher than the solvent boiling point, forming a solvent vapor layer that avoids the droplet to touch the hot substrate surface (Leidenfrost effect [40]), causing a randomly distributed deposition of micrometric/nanometric precursor particles on the surface. Since the substrate is also at a temperature above the organic precursor decomposition temperature, oxide formation initiates immediately during spray deposition, producing, if optimum deposition parameters are chosen [8], much more uniform and better quality films than the produced by spin coating.

From the considerations abovementioned concerning the organic precursor degradation temperature, it is of extreme importance to know in advance the physical chemical properties of the precursor salt. **Figure 4a** shows the Fourier-transform infrared spectra (FTIR) in attenuated reflectance mode (ATR) of zinc acetate dihydrate films treated at different temperatures, from 150 to 400°C. Peak (1) at 3377 cm^{-1} is from the asymmetric stretching mode of hydroxyl groups, whereas peaks (2) and (3) are from the stretching modes of the precursor ester groups (C=O and C—O, respectively). Peaks (4) and (5) are bending modes associated with the CH_3 groups and peaks (6) and (7) are due to bending modes of C=C bonds and COO^- groups, respectively. Peaks (8) and (9) correspond to Zn—OH and Zn—O stretching modes. One observes that the peaks associated to the organic phase of zinc acetate [10] gradually disappear by increasing the temperature, remaining only species associated with the inorganic phase (Zn—O) for temperatures above 400°C. Thermogravimetric analysis (**Figure 4b**) shows two main mass loss peaks, one around 100°C, due to loss of adsorbed water and water of crystallization and another around 290°C, due to the thermal degradation of the organic phase

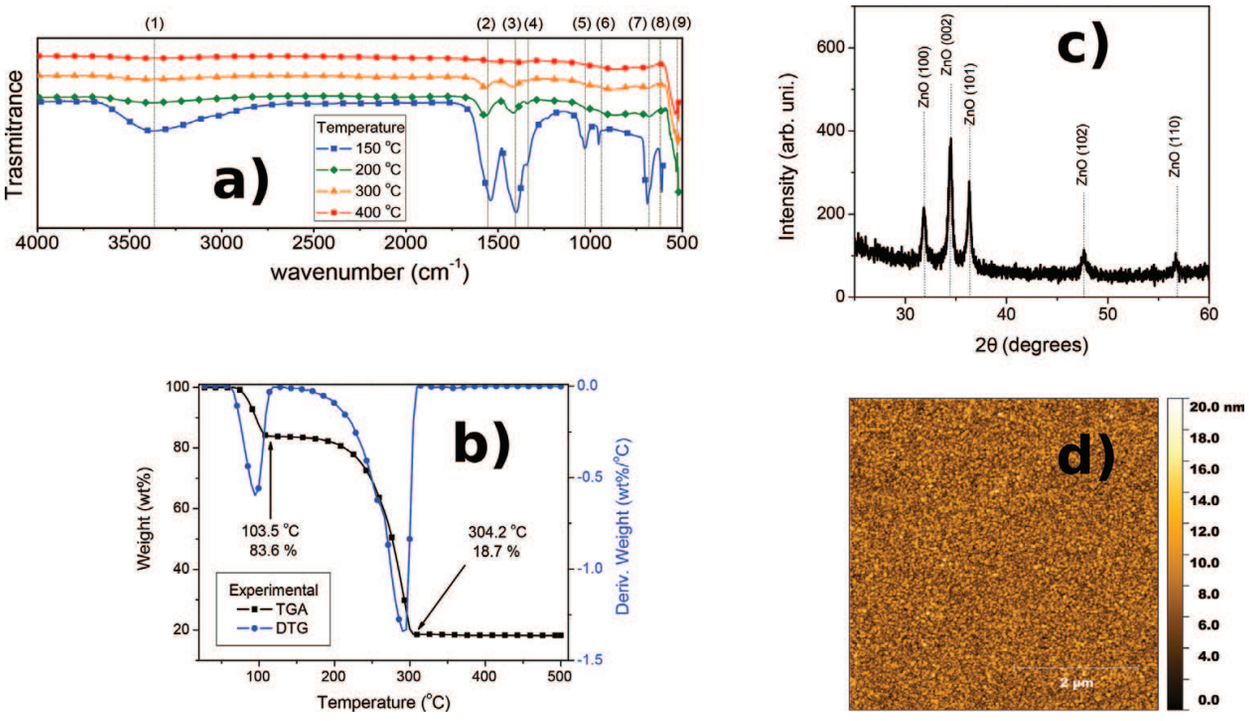

Figure 4. (a) Thermogravimetric analysis of zinc acetate; (b) FTIR spectra of zinc acetate at different temperatures; (c) DRX data from a spray-coated film at 350°C; and (d) AFM image of a spray-coated film.

of the precursor. Above 305°C, no significant mass loss is no longer observed up to 500°C, indicating that, probably, most of the remaining mass is due to the inorganic phase (ZnO).

The X-ray diffraction results shown in **Figure 4c** (obtained from a spray-coated sample deposited at 350°C) corroborate the expected results observed from FTIR and TGA/DTG analysis due to the typical pattern of the ordered hexagonal wurtzite phase (according to JCPDS Card No. 36-1451). Atomic force microscopy (AFM) of a spray-coated film at 350°C is shown in **Figure 4d** demonstrating the previously discussed uniform film morphology. Average surface roughness is less than 5 nm and observed rod-like structures have diameters inferior to 100 nm.

2.2.2. Metal oxide nanoparticles

Another interesting approach to obtain thin-film devices from solution is by the use of metal oxide nanoparticles which can be dispersed in water or organic solvents [5–7, 13]. The used nanoparticles are usually obtained by known inorganic synthesis methods and some options are commercially available. These nanoparticles can be used in the form of colloidal suspensions (which often need stabilizers to remain stable) to permit solution processing. The great advantage to use oxide nanoparticles is that the semiconducting phase is already present in the colloidal suspensions and deposition can be carried out at room temperature, without the need of further thermal treatment. This feature is important for the use of flexible substrates, which do not stand temperatures higher than 200°C. However, oxide nanoparticles suspensions usually give rise to lower quality films, with high roughness and large grain boundaries that are deleterious to the film electrical properties. Future improvements in the quality of films produced from oxide nanoparticles suspensions might improve device performance and make this alternative more interesting than processes involving the pyrolysis of organic precursor materials.

2.3. Thin-film transistors

Thin-film transistors are electronic devices in which all the active layers (semiconductor, electrodes and dielectric layer) are deposited as thin-films onto a supporting (non-active) substrate. The main role of the substrate in a TFT is to give mechanical support to the device structure and it does not interfere on the electrical characteristics of the transistor. The main use of this type of structure is as an electronic switch, having the current between two electrodes (drain and source) controlled (or modulated) by the voltage applied to a gate electrode which is separated from the drain and source electrodes by a highly insulating dielectric layer. Ideally, the current through the gate electrode (I_g) should be extremely small and could be neglected when compared to the current between the drain and source electrodes (I_{DS}), which can vary several orders of magnitude by varying the gate voltage (V_g). The drain-source current flows in the plane of the film direction, perpendicularly to the applied gate voltage, and is also dependent on the applied drain-source voltage (V_{DS}). Drain and source electrodes are usually formed by two long parallel metal stripes separated by a distance *L* known as *channel length*. The overlapping distance of the drain and source electrodes in the plane of the film is defined as the *channel width*, *w*.

From the point of view of the structure, TFTs can be constructed in diverse ways, with four basic distinct structures as depicted in **Figure 5**. The difference among these structures is the position of the electrodes relative to the active semiconducting layer. In a top-gate, bottom-contact (TGBC) configuration (**Figure 5a**) the gate electrode is the uppermost layer, on top of the dielectric layer, and the drain and source electrodes are the lowermost layers, being underneath the semiconducting layer. In this structure, drain and source electrodes can be deposited by lift-off photolithography or shadow mask thermal evaporation directly onto the substrate. Another characteristic of this structure is that the insulating layer must be deposited onto the semiconducting layer, a condition which cannot be achieved, depending on the deposition method of the dielectric material. Top-gate, top-contact (TGTC) configuration (**Figure 5b**) is similar to TGBC configuration with the difference that the drain and source electrodes are deposited onto the semiconducting layer. This configuration has also the same limitations concerning the dielectric layer deposition as the TGBC. Bottom-gate configurations (**Figure 5c** and **d**) are interesting from the point of view that they have three common stages (substrate, gate electrode and dielectric layer) and are very convenient when only the semiconducting active layer is changed (particularly for bottom-gate, bottom-contact, BGBC). However, bottom gate structures are not appropriate for use when the dielectric layer does not support temperatures higher than the deposition temperature of the semiconducting layer or does not resist to the solvent used to deposit the active layer.

Thin-film transistors have the electrical performance evaluated mainly by two characteristic current–voltage curves, namely, the *output* and the *transfer* curves. The output curve is defined by the drain-source current (I_{DS}) versus the drain-source voltage (V_{DS}) at different constant values of the gate voltage (V_g), whereas the transfer curve is obtained by measuring I_{DS} *versus* V_g at different constant values of V_{DS}. In a TFT configuration, the channel conductance (between drain and source electrodes) depends on the amount of free charge carriers present in the transistor channel, which can be controlled by the application of a bias voltage at the gate electrode.

If the semiconducting material is n-type, free electrons are accumulated next to the semiconductor/dielectric interface when a positive voltage is applied at the gate electrode (respective to the

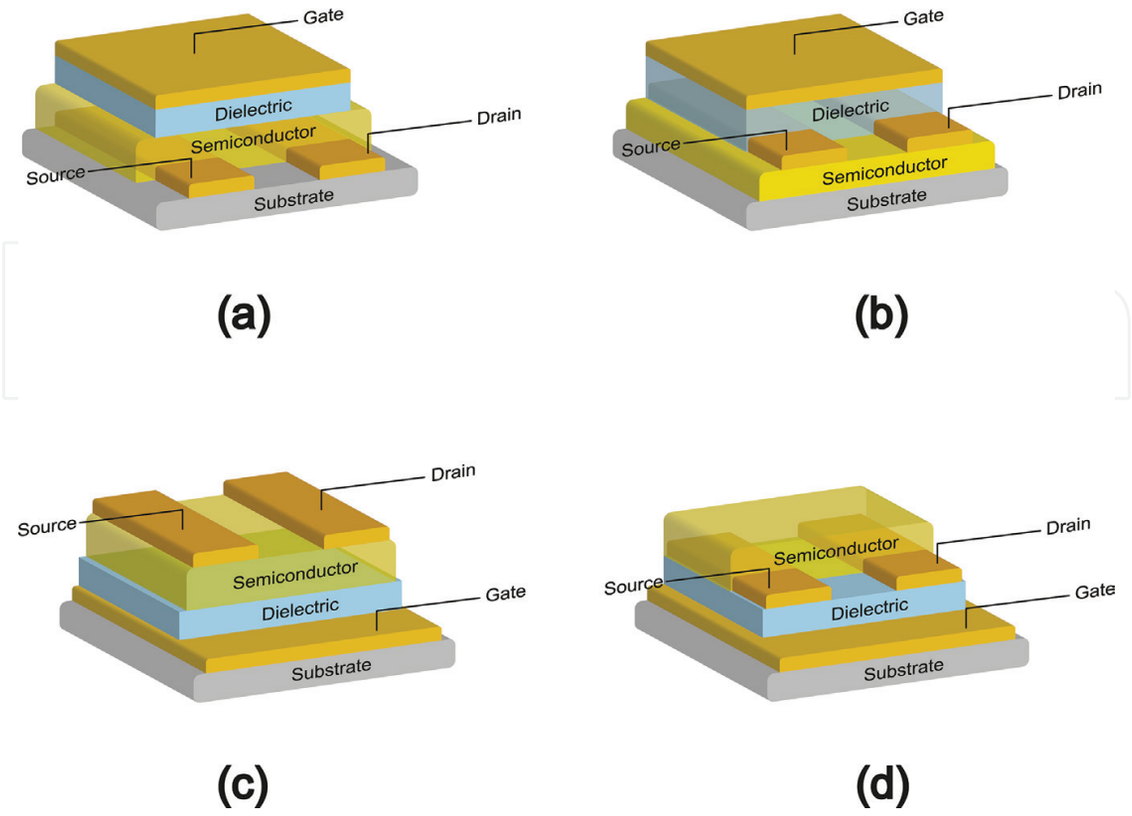

Figure 5. Most common electrode configuration for thin-film transistors: (a) top-gate, bottom-contact; (b) top-gate, top-contact; (c) bottom-gate, top-contact and (d) bottom-gate, bottom-contact.

source electrode), increasing the channel conductance (accumulation regime). The higher the positive gate bias, the more conductive becomes the transistor channel. However, for a negative gate bias, free electrons are repelled from the semiconductor/dielectric interface, decreasing the density of free charge carriers in the transistor channel (depletion regime) and, consequently, reducing the channel conductance. As a consequence, the channel current for a negative V_g is almost negligible when compared to the current for a positive V_g. For a p-type semiconductor, the majority free charge carriers are holes and the transistor is in the accumulation regime (conductive channel) when a negative bias is applied to the gate electrode and in depletion regime (resistive channel) when a positive bias is applied to the gate electrode.

The dependence of I_{DS} on V_{DS}, for low values of V_{DS}, is approximately linear, since, for a fixed value of V_g much higher than V_{DS} and in the absence of fixed charged defects at the semiconductor/dielectric interface, the channel majority free charge carrier distribution is nearly uniform. As the value of V_{DS} increases, the I_{DS} starts to deviate from the linear behavior (toward a sublinear behavior) since the charge near the drain electrode is reduced by the semiconductor potential. At a certain drain-source voltage, the accumulated charge next to the drain electrode is reduced near to zero, forming what is called the *pinch-off* point, which moves toward the source electrode as V_{DS} continues to increase. However, the voltage at the pinch-off point remains nearly constant. Therefore, the amount of charge that arrives at the pinch-off point remains the same (as well as the channel current) when a voltage beyond the formation of the pinch-off point (V_{sat}) is applied, despite the reduction on the effective channel length.

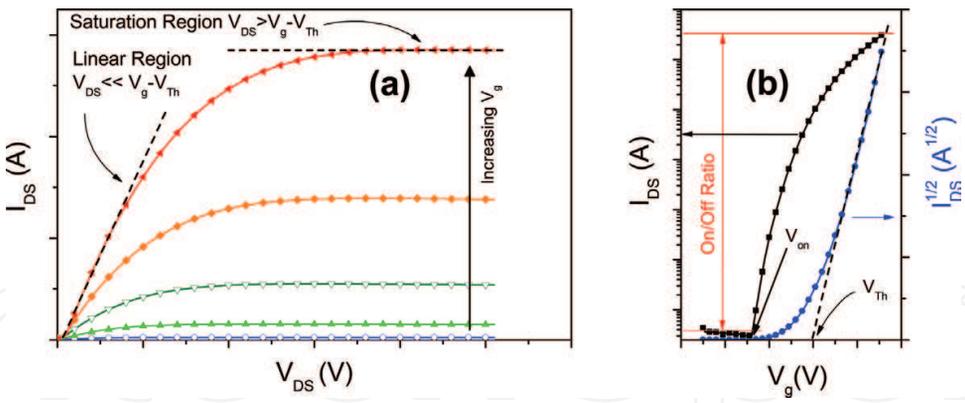

Figure 6. Characteristic curves of TFTs (a) output curves with characteristic linear and saturation regions; (b) transfer curve and $I^{1/2}$ versus vg (linear scale) extrapolation of Vth and slope for saturation mobility determination;.

This means that, for V_{DS} higher than V_{sat}, the channel current achieves a saturation regime, as observed in the output curves of **Figure 6a**.

The drain-source current in the linear regime can be approximated by [41, 42]:

$$I_{DS,\ lin} = \frac{w\mu C_{ox}}{L}\left(V_g - V_{th} - \frac{V_{DS}}{2}\right)V_{DS} \quad for\ V_{DS} \ll \left(V_g - V_{th}\right) \tag{1}$$

where μ is the charge carrier mobility, C_{ox} is the capacitance per unit area of gate dielectric layer ($C_{ox} = C/A = k\varepsilon_0/d$, with ε_0 the vacuum electric permittivity, k, the dielectric constant of the insulating layer and d, its thickness) and V_{th} is the *threshold voltage*, a voltage associated to the presence of charged traps at the semiconductor/dielectric interface and the difference of the work function between the semiconductor and the dielectric material, which is necessary to achieve the flat-band condition in the transistor channel. The channel current in the saturation regime, on the other hand, can be given by [41, 42]:

$$I_{DS,\ sat} = \frac{w\mu C_{ox}}{L}\left(V_g - V_{th}\right)^2 \quad for\ V_{DS} \gg \left(V_g - V_{th}\right) \tag{2}$$

Eq. (2) means that the square root of the channel current depends linearly on the gate voltage. Consequently, a plot of $(I_{DS})^{1/2}$ versus V_g (curve in blue in **Figure 6b**) may give a straight line which intercepts the abscissa at V_{th} and which slope gives the transistor *transconductance*, g_m:

$$g_m = \left[\frac{\partial\sqrt{I_D}}{\partial V_g}\right]_{V_{DS}=cte} \tag{3}$$

Combining with Eq. (2), the carrier mobility in the saturation regime can be calculated:

$$\mu_{sat} = \frac{2L\left(\frac{\partial\sqrt{I_D}}{\partial V_g}\right)^2}{w\,C_{ox}} \tag{4}$$

Even though the carrier mobility in a TFT can be obtained in different conditions, the saturation regime is very important on the transistor operation, the reason why most of the papers use the saturation mobility as one of the relevant parameters (along with V_{th}) used to evaluate the transistor performance.

Considering that TFTs can be used as electronic switches, other electrical parameters concerning the switching capacity are also used to evaluate the transistor performance: (1) the *on/off ratio* (I_{on}/I_{off}); (2) the onset voltage (V_{on}) and (3) the subthreshold swing (SS). The on/off ratio, which extraction method is shown in the transfer curve of **Figure 6b**, represents the ratio between the channel currents when the transistor is in the conduction mode (*Ion*) and when it is switched off (I_{off}). Since the ideal I_{off} value is minimal (to avoid power consumption when not operating), I_{on}/I_{off} should be the highest as possible. Typical good values for on/off ratio are above 10^5–10^6. The onset voltage is defined as the gate voltage necessary for the transistor switch from the "off state" to the "on state" and can be directly determined from the transfer curve as shown in **Figure 6b**. The subthreshold voltage (which is measured in volts/decade) is defined by:

$$SS = \left[\frac{\partial V_g}{\partial \log(I_{DS})}\right]_{min} \quad (5)$$

and can also be determined from the transfer curve data. It gives the information on how much gate voltage in needed to make the drain-source current increase by a factor of 10. Thus, the lowest this value, the better is the transistor performance.

2.3.1. Solution-processed ZnO TFTs

In the present section, we compare the results from the electrical characterization of ZnO TFTs with the active deposited by spray-pyrolysis and by spin-coating, annealed at different temperatures (300 and 500°C) after deposition. **Figure 7a–d** shows the output curves of the produced devices. Substrates are p-type (Boron) doped Si wafers with a thermally grown SiO_2 insulating layer (100 nm thick) used in a bottom-gate structure. Aluminum top drain and source electrodes were deposited on top of the ZnO layer, with a channel width of 5 mm and a channel length of 100 μm (*w*/*L* ratio of 50).

The output curves show that spray-coated devices present better transistor characteristics compared to spin-coated transistors. Operating currents of spray-coated devices are considerably higher (more than 7 times for devices annealed at 300 oC and more than 13 times for devices annealed at 500 oC) than the operating currents observed for devices produced by spin-coating. Moreover, spin-coated devices have much higher off currents (for $V_g = 0$ V), probably due to higher lateral leakage current (spin-coated films cover the whole substrate area whereas spray-coated films can be deposited selectively in a smaller active area) and/or higher leakage current through the gate dielectric (due to Leidenfrost effect, spray-pyrolysis deposition promote less cracks in the insulating SiO_2 bottom layer than spin-coating).

The transfer curves (**Figure 7e** and **f**) also show strong dependence on deposition method and annealing temperature. Spray-coated devices, as expected from the output curves, present much higher on/off ratios (about 10^6 against 10^3) and also saturation mobility values almost 10 times higher than spin-coated TFTs. Subthreshold swing (SS) values of spray-coated TFTs are smaller and do not present significant variation on annealing temperature as observed for spin-coating. Improved device characteristics of spray-coated devices can be explained by better film quality and crystallinity, which promotes less charge trapping and scattering. The temperature influence on the transfer curves for devices produced by the same deposition method indicates that at higher temperatures the semiconductor intrinsic conductivity increases due to more efficient elimination of organic residues and better film crystallinity.

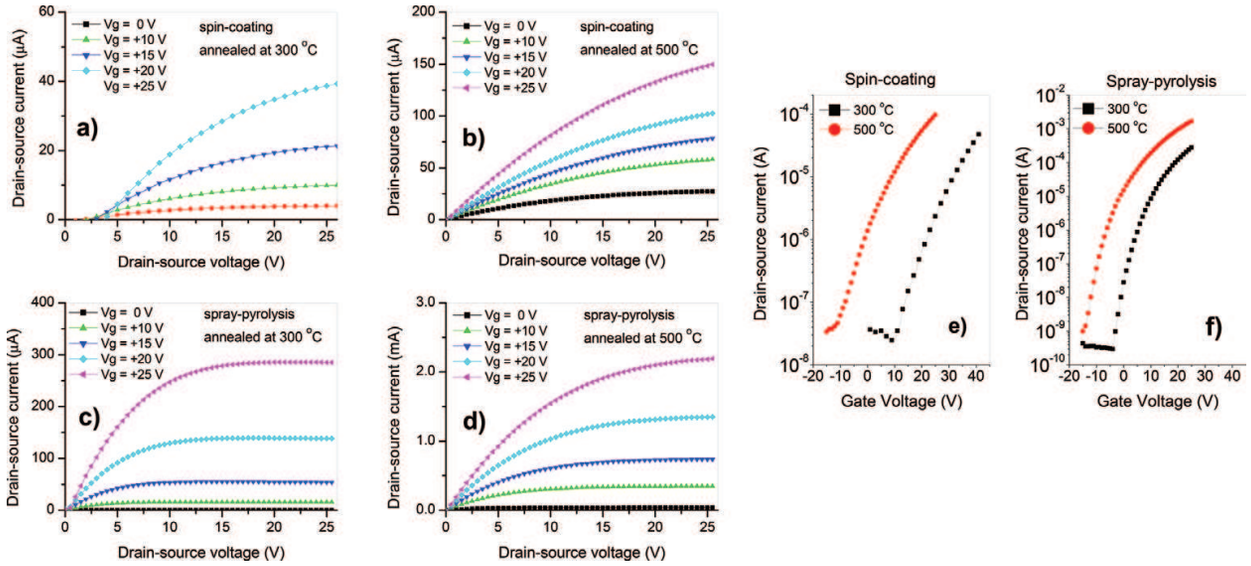

Figure 7. Output curves for solution-processed ZnO TFTs prepared by spin-coating and spray-pyrolysis and annealed at temperatures. Transfer curves for a spin-coated and spray-coated TFTs annealed at different temperatures.

Deposition method/ Annealing temperature	μ_{sat} ($cm^2.V^{-1}.s^{-1}$)	V_{th} (V)	V_{on} (V)	I_{on}/I_{off}	SS (V/dec)
Spin-coating/ 300 °C	0.14	+10.0	+10.1	1.3×10^3	2.91
Spin-coating/ 500 °C	0.36	+4.5	-12.3	3.0×10^3	6.37
Spray-coating/ 300 °C	1.29	+10.0	+3.3	1.3×10^6	2.00
Spray-coating/ 500 °C	5.55	+4.5	-14.5	2.1×10^6	2.13

Table 1. Electrical parameters obtained from the TFT data presented on **Figure 7**.

Higher intrinsic conductivity decreases both the threshold and the onset voltages, since more negative voltages are needed to deplete the transistor channel from intrinsic n-type charge carriers. **Figure 7e** also shows that higher annealing temperatures promote the reduction of electron traps at the semiconductor/dielectric interface, which are responsible to displace V_{th} and V_{on} to positive values. **Table 1** summarizes the electrical parameters obtained from the curves presented on **Figure 7**.

2.3.2. TFTs based on ZnO-related compounds

The electrical properties of solution processed ZnO films can change dramatically by incorporating other metallic elements in the precursor solution, obtaining doped ZnO or ternary or quaternary metal oxide alloys. When a small amount of a precursor as aluminum acetate dibasic (**Figure 3b**) is added to a zinc acetate solution, aluminum-doped zinc oxide (AZO) films can be obtained after precursor pyrolysis. Aluminum atoms can substitute zinc atoms in the crystalline lattice, originating a donor level close to the conduction band, increasing the material conductivity by doping.

http://dx.doi.org/10.5772/intechopen.78221

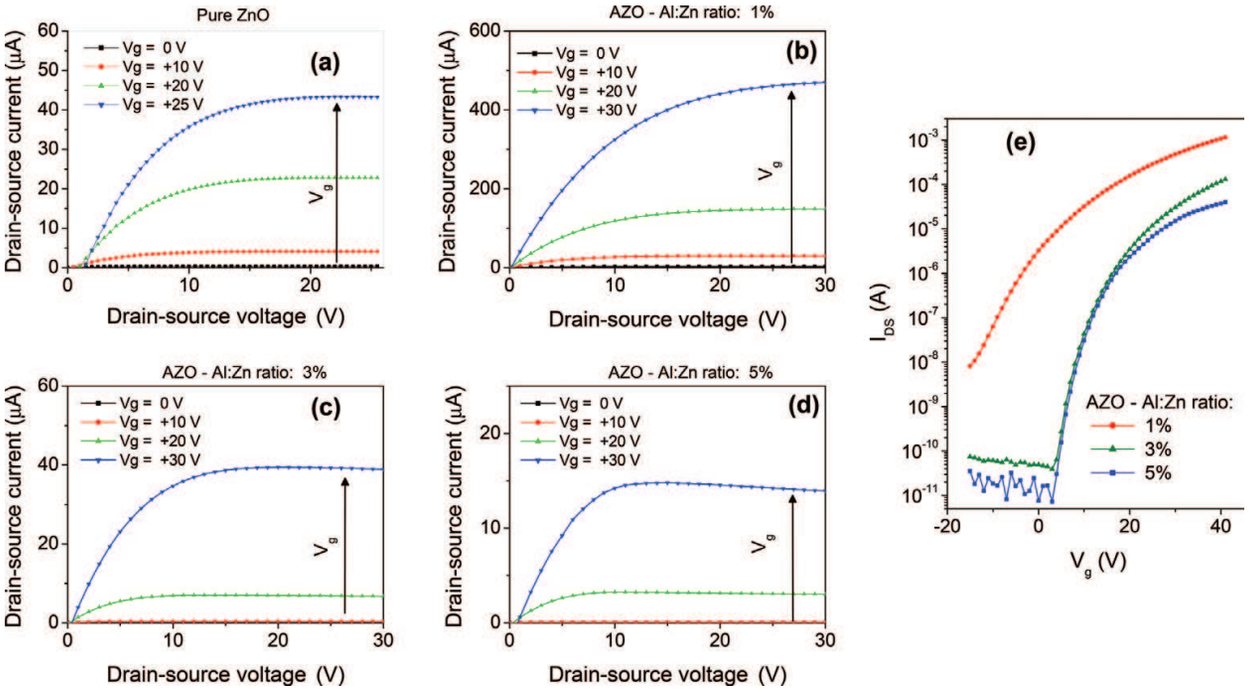

Figure 8. Output (a–d) and transfer (e) curves from spin-coated AZO TFTs produced using different active layer compositions.

Figure 8 depicts the characteristic TFT curves of spin-coated AZO devices produced using Al:Zn ratios which varied from 0% (pure ZnO) to 5%. One observes that a small addition of Al (1%) is responsible for a substantial increase (more than 10 times) on the operating current when compared to a pure ZnO TFT, corroborating the expectation of semiconductor doping. By increasing the Al concentration, however, the device current gradually decreases (for 5%, the currents are smaller than for pure ZnO). At Al concentrations equal and higher than 10%, the currents became so small that transistor characteristics could not even be observed. Such behavior can be explained that, for higher Al concentrations, the formation of insulating aluminum-related compounds (like aluminum oxide) becomes more efficient than the semiconductor doping, and the phase separation between semiconducting and insulating regions leads to poorer morphological properties of the film, reducing the overall conductivity.

The transfer curves of **Figure 8e** show that the TFT with 1% AZO active layer has a higher on current (and, consequently, higher mobility in saturation) and a higher intrinsic conductivity as well, which affects negatively the threshold voltage and the on/off ratio. At this point, it is important to notice that to obtain good TFT performance, it is not important to only increase the material conductivity, but also improve the film quality and control the number of defects at the semiconductor/dielectric interface.

The addition of a precursor like indium acetate hydrate (**Figure 3c**) to a zinc precursor solution does not cause doping like in AZO (differently than Al, In atoms do not substitute Zn atoms in the lattice), but the formation of a ternary compound, indium zinc oxide (IZO). In ternary compounds, the relative concentration metal atoms must be much higher compared to doped compounds to result on significant changes in the electrical properties of the material. **Figure 9a** and **b** show the

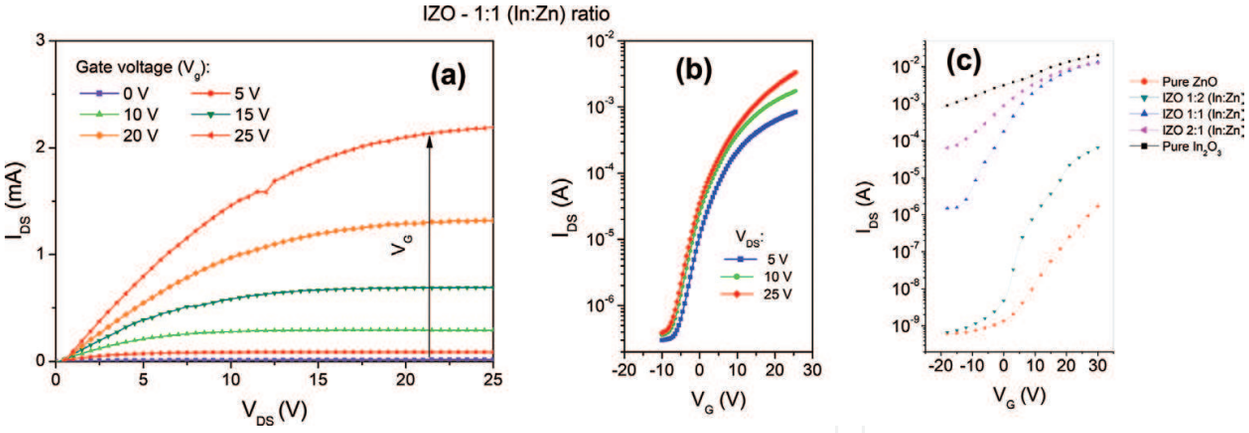

Figure 9. Output (a) and transfer (b) curves for a spin-coated IZO (1:1) TFT; (c) transfer curves for spin-coated TFTs at different IZO/ZnO compositions.

characteristic curves of a spin-coated IZO TFT using a 1:1 In:Zn molar ratio and treated at 350°C. It presents much improved TFT properties when compared to a ZnO TFT fabricated using similar processing method (**Figure 7a**). A saturation mobility of 5.32 $cm^2\ V^{-1}\ s^{-1}$ and an on/off ratio of 4.3×10^4 is obtained, against 0.14 $cm^2V^{-1}\ s^{-1}$ and 1.3×10^3 for the pure ZnO TFT (first row of **Table 1**). Spray-coated TFTs comprising IZO layer were not produced due to the need of optimization of the spray deposition method for the solvent (2-methoxyethanol). However, the expectation is to obtain transistors with much superior performance by using spray-pyrolysis IZO active layer.

The transfer curves of TFTs comprising different active layers (pure ZnO, pure indium oxide and IZO at 1:2, 1:1 and 2:1 In:Zn molar ratios) are presented in **Figure 9c**. A gradual increase on the on current (and on the saturation mobility) is observed when the indium concentration increases from pure ZnO up to 1:1 In:Zn. For higher In concentrations, the increase in the on current is not significant. However, the off current (and the intrinsic conductivity as well) always increase with the indium concentration. As a result, the transistor performance improves due to the increase of the mobility until a In:Zn molar ratio of 1:1, but deteriorates for higher indium concentrations due to decrease of the on/off ratio and displacement of V_{th} and V_{on} toward negative values. Once again, we observe that a too conductive material like pure indium oxide does not result on superior performance transistor. As observed in **Figure 9c**, the pure indium oxide transistor has a too low on/off ratio and is not suitable for switching applications.

2.3.3. Atmosphere influence on TFT performance

In Section 2.1 we discussed briefly about the nature of the native defects which are responsible to the n-type character of ZnO. Theoretical calculations demonstrate that oxygen vacancies cannot be responsible for the unintentional n-doping of ZnO [12, 34, 35, 39]. However, reports on the increase of conductivity by increasing the oxygen pressure during sputtering deposition [14, 28, 40] are frequently mentioned as evidence that they play a key role in metal oxides n-type conductivity.

Atmospheric oxygen can also influence the electrical properties of ZnO TFTs even after the device manufacture. In **Figure 10a**, the transfer curves of a spray-coated ZnO TFT deposited at 350°C are presented as a function of exposure time in air. Previously to the experiment, the samples were annealed, in vacuum, at 150°C, for 1 h. Although differences in the electrical

http://dx.doi.org/10.5772/intechopen.78221

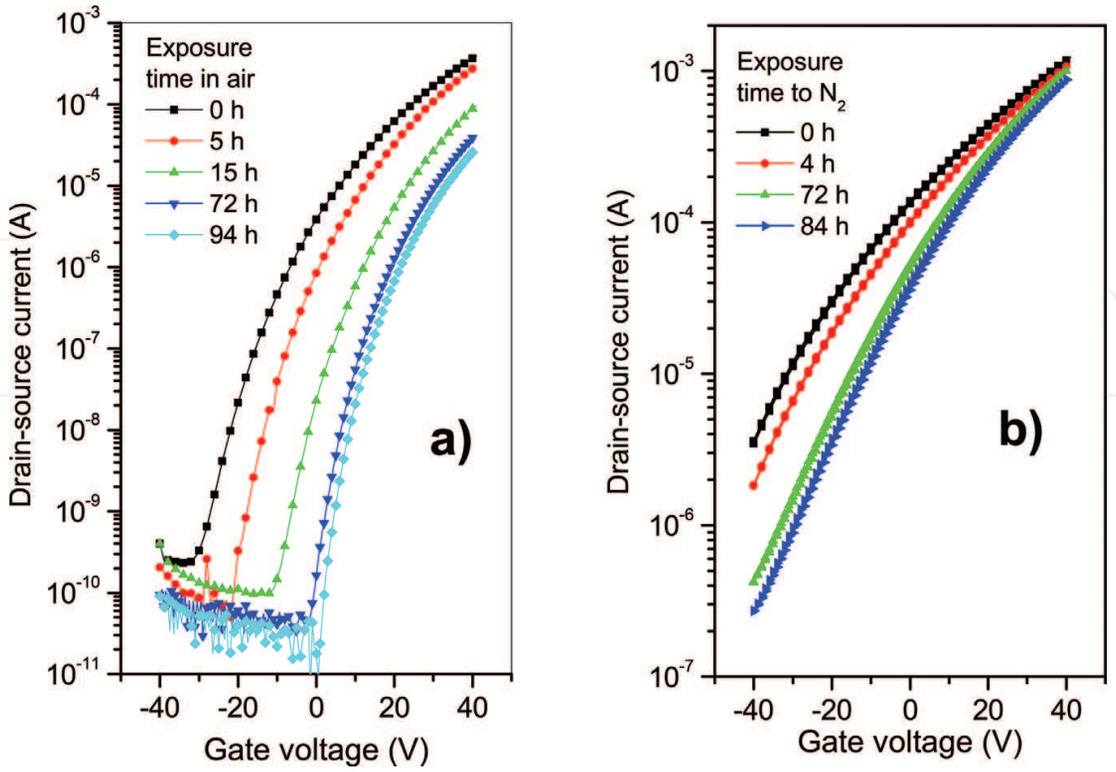

Figure 10. Transfer curves for a spray-coated ZnO TFT in different atmospheres: (a) in air; (b) in N_2, with H_2O and O_2 levels below 10 ppm (glove-box).

measurements could not be observed for short time intervals like few minutes, a significant change can be observed after 5 h in air. Both the intrinsic and on current continuously decrease as a function of time until about 40 h in air. After 40 h, the transfer curve seems to stabilize, with no substantial change until 94 h. **Figure 10b** shows the transfer curves for another transistor which was fabricated and annealed according the same conditions, but it was left inside a glove-box, with oxygen and water content lower than 10 ppm. The transfer curves show a slight variation in the first few hours, but also stabilize after about 40 h in N_2 atmosphere.

Figure 11 presents the evolution in time of the saturation mobility and the threshold voltage for the transistor exposed to air and for the transistor left in inert atmosphere (N_2). The variation in both parameters was higher for the transistor exposed to air. Moreover, the saturation mobility decreases when exposed to air and, in N_2, presents a small increase in the first 24 h. The threshold voltage, in both cases, shifts toward positive values. However, in N_2, it is still negative whereas, in air, it is positive. Negative V_{th} values in n-type TFTs are more associated to the increase of the intrinsic conductive than to the presence of charged defects. On the other hand, positive values of V_{th} in a n-type semiconductor is better explained by charge traps at the semiconductor/dielectric interface.

The significant variation on the electrical behavior of the ZnO TFT by exposure to oxygen rich atmosphere cannot be used, however, as evidence that the electron conductivity in ZnO is due to oxygen vacancies. Adsorbed atmospheric oxygen species can actually act as electron traps in ZnO, decreasing the electrical conductivity, but this effect can occur independently on which native defect generate free n-type charge carriers.

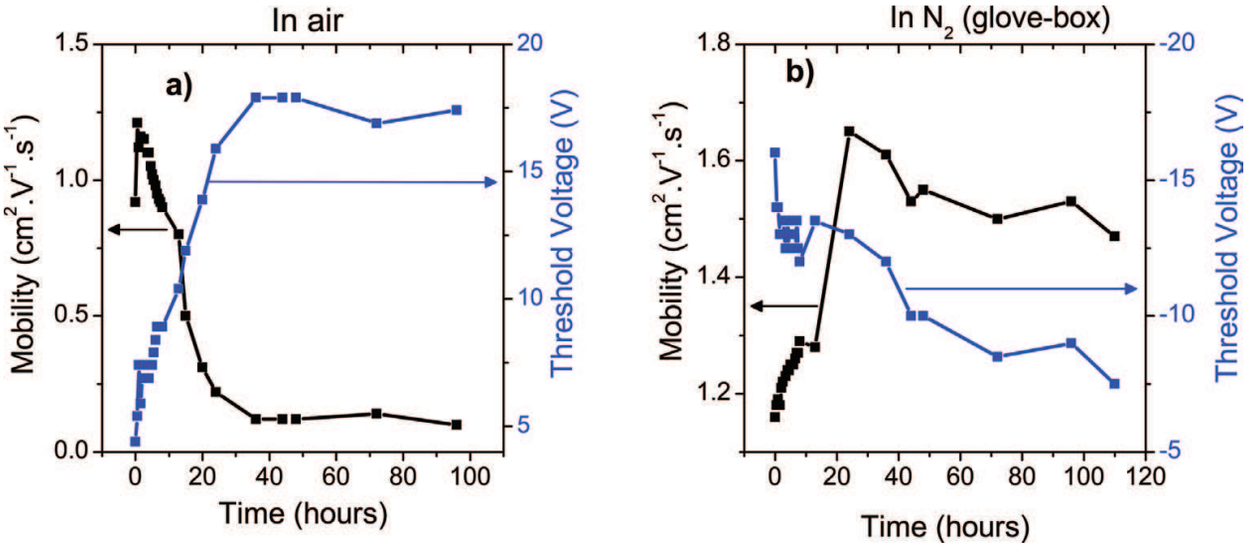

Figure 11. Time dependence of the mobility and threshold voltage for a spray-coated ZnO TFT in different atmospheres: (a) in air; (b) in N_2, with H_2O and O_2 levels below 10 ppm (glove-box).

2.3.4. TFT photoresponse in the UV range

The wide bandgap of zinc oxide (E_g ~ 3.37 eV) makes it a suitable UV sensing material since its response is not affected by visible light, differently to, for example, Si-based photosensors [32, 43–45]. Another interesting feature of ZnO-based devices is the occurrence of persistent photoconductive, that is, the material conductivity remains higher than the dark conductive even several hours after UV-light exposure. **Figure 12** shows this effect on a spray-coated ZnO TFT deposited at 350°C. The transistor was irradiated for 2 min by a UV LED (peak at 355 nm, irradiance of 68 μW/cm²) and then several transfer curves were recorded in a 6 h interval. The experiment shows that the saturation mobility increases more than 3 times and the threshold voltage shifts almost 15 V toward negative voltages by UV irradiation, taking more than 6 h return to the original values.

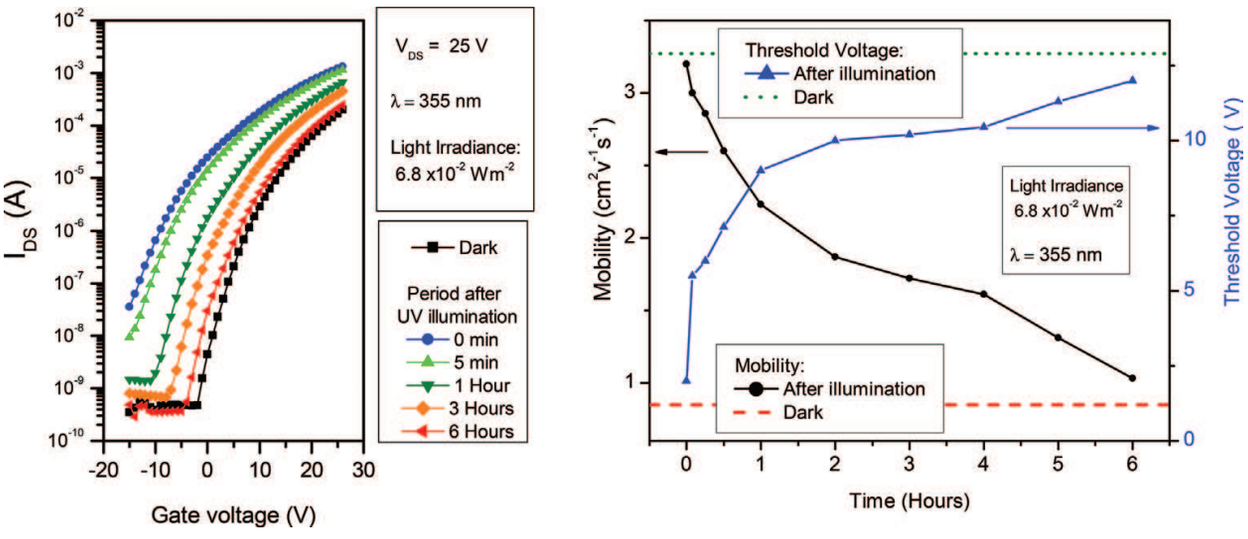

Figure 12. Electrical characteristics of ZnO TFT after UV exposure in air.

http://dx.doi.org/10.5772/intechopen.78221

Such effects can be explained by the adsorption of atmospheric species, specially molecular oxygen, to the film surface. As described in the previous section, oxygen from the air adsorbs to the ZnO surface and acts as free electrons traps, decreasing the semiconductor conductivity. The photogeneration of electron–hole pairs causes the release of the adsorbed O_2 molecule by the recombination of the trapped electrons with the photogenerated holes [38], leaving free electrons in the bulk and, consequently, increasing the conductivity. The slow readsorption of oxygen molecules from the air is, therefore, the main mechanism behind the persistent photoconductivity effect observed in ZnO TFTs.

3. Conclusions

We made a brief review on the basic properties of semiconducting metal oxides and presented the advantages of using solution-processed metal oxides films as the active layer of high-performance thin-film transistors for transparent, low-cost and large-area applications. The presented results from ZnO TFTs indicate that spray-pyrolysis deposition has an enormous potential to provide devices with improved performance when compared to other deposition methods like spin coated, suggesting that further improvement can be achieved by using doped or ternary ZnO-related compounds like AZO or IZO. The observed dependence of the electrical properties of ZnO TFTs on the environment oxygen content and on the UV-light exposure endorse them as excellent candidates for gases, volatile compounds or UV-radiation sensors. The fact that ZnO TFTs present sensing responses that can be quantified by multiple parameters (μ_{sat}, V_{on}, V_{th}, I_{on}/I_{off}, SS, etc.) is a great advantage compared to the commonly proposed sensing units which usually present variations in a single parameter (like resistance, conductance or capacitance).

Acknowledgements

The authors acknowledge the financial support from CNPq (scholarships from Molecular Biophysics graduate program, IBILCE/UNESP), FAPESP (grant # 2013/24461-7) and to the contribution from State University of São Paulo—UNESP (PROPe/PROPG), which made possible the publication of this work. We also thank Nanotechnology National Laboratory for Agriculture – LNNA (CNPq/SISNANO/MCTI) for the XRD measurements.

Author details

João P. Braga[1], Guilherme R. De Lima[1], Giovani Gozzi[2] and Lucas Fugikawa Santos[2]*

*Address all correspondence to: lucas.fugikawa@unesp.br

1 Physics Department, IBILCE, São Paulo State University (UNESP), São José do Rio Preto, SP, Brazil

2 Physics Department, IGCE, São Paulo State University (UNESP), Rio Claro, SP, Brazil

References

[1] Kwack YJ, Choi WS. Solution-processed zinc-tin-oxide thin-film transistor by electrohydrodynamic spray. Electronic Materials Letters. 2012;**8**:341-344. DOI: 10.1007/s13391-012-1069-3

[2] Adamopoulos G, Bashir A, Wöbkenberg PH, Bradley DDC, Anthopoulos TD. Electronic properties of ZnO field-effect transistors fabricated by spray pyrolysis in ambient air. Applied Physics Letters. 2009;**95**:133507. DOI: 10.1063/1.3238466

[3] Li CS, Li YN, Wu YL, Ong BS, Loutfy RO. Performance improvement for solution-processed high-mobility ZnO thin-film transistors. Journal of Physics D: Applied Physics. 2008;**41**:125102. DOI: 10.1088/0022-3727/41/12/125102

[4] Krunks M, Mellikov E. Zinc oxide thin films by the spray pyrolysis method. Thin Solid Films. 1995;**270**:33-36. DOI: 10.1016/0040-6090(95)06893-7

[5] Lim SC, Oh JY, Koo JB, Park CW, Jung S-W, Na BS, Chu HY. Electrical properties of solution-deposited ZnO thin-film transistors by low-temperature annealing. Journal of Nanoscience and Nanotechnology. 2014;**14**:8665-8670. DOI: 10.1166/jnn.2014.10002

[6] Oh J-Y, Kang S-Y, Hwang C-S, Kim G-H, Ahn SD, Kim C-A, Koo JB, Suh K-S, Shim H-K. P-28: ZnO TFTs fabricated at room temperature by solution process. SID Symposium Digest of Technical Papers. 2008;**39**:1274. DOI: 10.1889/1.3069371

[7] Jun JH, Park B, Cho K, Kim S. Flexible TFTs based on solution-processed ZnO nanoparticles. Nanotechnology. 2009;**20**:505201. DOI: 10.1088/0957-4484/20/50/505201

[8] de Lima GR, Braga JP, Gozzi G, and Santos LF. Optimization of the electrical performance of metal oxide thin-film transistors by varying spray deposition parameters. MRS Advances. 2018;**3**:247-253. DOI: 10.1557/adv.2018.35

[9] Meyers ST, Anderson JT, Hung CM, Thompson J, Wager JF, Keszler DA. Aqueous inorganic inks for low-temperature fabrication of ZnO TFTs. Journal of the American Chemical Society. 2008;**130**:17603-17609. DOI: 10.1021/ja808243k

[10] Martins DE, Gozzi G, Santos LF. Influence of spray-pyrolysis deposition parameters on the electrical properties of aluminium zinc oxides thin films. MRS Advances. 2018;**3**:283-289. DOI: 10.1557/adv.2018.121

[11] Md Sin ND, Mamat MH, Mohammad RM. Optical properties of nanostructured aluminum doped zinc oxide (ZnO) thin film for thin film transistor (TFT) application. Advances in Materials Research. 2013;**667**:511-515. DOI: 10.4028/www.scientific.net/AMR.667.511

[12] Lin M-L, Huang J-M, Ku C-S, Lin C-M, Lee H-Y, Juang J-Y. High mobility transparent conductive Al-doped ZnO thin films by atomic layer deposition. Journal of Alloys and Compounds. 2017;**727**:565-571. DOI: 10.1016/j.jallcom.2017.08.207

[13] Diallo AK, Gaceur M, Fall S, Didane Y, Ben Dkhil S, Margeat O, Ackermann J, Videlot-Ackermann C. Insight about electrical properties of low-temperature solution-processed Al-doped ZnO nanoparticle based layers for TFT applications. Materials Science and Engineering B. 2016;**214**:11-18. DOI: 10.1016/j.mseb.2016.07.015

[14] Walker DE, Major M, Yazdi MB, Klyszcz A, Haeming M, Bonrad K, Melzer C, Donner W, von Seggern H. High mobility indium zinc oxide thin film field-effect transistors by semiconductor layer engineering. ACS Applied Materials & Interfaces. 2012;**4**:6835-6841. DOI: 10.1021/am302004j

[15] Park SM, Lee DH, Lim YS, Kim DK, Yi M. Effect of aluminum addition to solution-derived amorphous indium zinc oxide thin film for an oxide thin film transistors. Microelectronic Engineering. 2013;**109**:189-192. DOI: 10.1016/j.mee.2013.03.121

[16] Kim GH, Kim HS, Shin HS, Du Ahn B, Kim KH, Kim HJ. Inkjet-printed InGaZnO thin film transistor. Thin Solid Films. 2009;**517**:4007-4010. DOI: 10.1016/j.tsf.2009.01.151

[17] Yoon S, Kim SJ, Tak YJ, Kim HJ. A solution-processed quaternary oxide system obtained at low-temperature using a vertical diffusion technique. Scientific Reports. 2017;**7**:43216. DOI: 10.1038/srep43216

[18] Liu F, Qian C, Sun J, Liu P, Huang Y, Gao Y, Yang J. Solution-processed lithium-doped zinc oxide thin-film transistors at low temperatures between 100 and 300 °C. Applied Physics A: Materials Science & Processing. 2016;**122**:311. DOI: 10.1007/s00339-016-9903-3

[19] Zhang X, Zhai J, Yu X, Zhu R, Zhang W. Effect of annealing temperature on the performance of SnO_2 thin film transistors prepared by spray pyrolysis. Journal of Nanoscience and Nanotechnology. 2015;**15**:6183-6187. DOI: 10.1166/jnn.2015.10198

[20] Thomas SR, Pattanasattayavong P, Anthopoulos TD. Solution-processable metal oxide semiconductors for thin-film transistor applications. Chemical Society Reviews. 2013;**42**: 6910. DOI: 10.1039/c3cs35402d

[21] Perednis D, Gauckler LJ. Thin film deposition using spray pyrolysis. Journal of Electroceramics. 2005;**14**:103-111. DOI: 10.1007/s10832-005-0870-x

[22] Fortunato EMC, Barquinha PMC, Pimentel ACMBG, Gonçalves AMF, Marques AJS, Martins RFP, Pereira LMN. Wide-bandgap high-mobility ZnO thin-film transistors produced at room temperature. Applied Physics Letters. 2004;**85**:2541-2543. DOI: 10.1063/1.1790587

[23] Nomura K, Takagi A, Kamiya T, Ohta H, Hirano M, Hosono H. Amorphous oxide semiconductors for high-performance flexible thin-film transistors. Japanese Journal of Applied Physics. 2006;**45**:4303-4308. DOI: 10.1143/JJAP.45.4303

[24] Martins R, Barquinha P, Ferreira I, Pereira L, Gonçalves G, Fortunato E. Role of order and disorder on the electronic performances of oxide semiconductor thin film transistors. Journal of Applied Physics. 2007;**101**:44505. DOI: 10.1063/1.2495754

[25] Fortunato E, Barquinha P, Martins R. Oxide semiconductor thin-film transistors: A review of recent advances. Advanced Materials. 2012;**24**:2945-2986. DOI: 10.1002/adma.201103228

[26] Shi P, Huang L, Cui G, Zhang S, Zhang Y, Dong J, Yu W, Wang Y, Han D, Cong Y, Zhang X. High mobility transparent flexible nickel-doped zinc oxide thin-film transistors with small subthreshold swing. Electronics Letters. 2015;**51**:1595-1596. DOI: 10.1049/el.2015.2041

[27] Nomura K, Ohta H, Ueda K, Kamiya T, Hirano M, Hosono H. Thin-film transistor fabricated in single-crystalline transparent oxide semiconductor. Science. 2003;**300**:1269-1272. DOI: 10.1126/science.1083212

[28] Morkoc H, Ozgur U. General properties of ZnO. In: Zinc Oxide. Fundamentals, Materials and Device Technology. Weinheim, Germany: Wiley-VCH Verlag GmbH & Co. KgaA; 2009. pp. 1-76. DOI: 10.1002/9783527623945.ch1

[29] Tsakonas C, Kuznetsov VL, Cranton WM, Kalfagiannis N, Abusabee KM, Koutsogeorgis DC, Abeywickrama N, Edwards PP. Low temperature sputter-deposited ZnO films with enhanced hall mobility using excimer laser post-processing. Journal of Physics D: Applied Physics. 2017;**50**:485306. DOI: 10.1088/1361-6463/aa9316

[30] Fortunato E, Pereira L, Barquinha P, Ferreira I, Prabakaran R, Gonçalves G, Gonçalves A, Martins R. Oxide semiconductors: Order within the disorder. Philosophical Magazine. 2009;**89**:2741-2758. DOI: 10.1080/14786430903022671

[31] Look DC, Farlow GC, Reunchan P, Limpijumnong S, Zhang SB, Nordlund K. Evidence for native-defect donors in n-type ZnO. Physical Review Letters. 2005;**95**:225502. DOI: 10.1103/PhysRevLett.95.225502

[32] Look DC. Progress in ZnO materials and devices. Journal of Electronic Materials. 2006;**35**:1299-1305. DOI: 10.1007/s11664-006-0258-y

[33] Özgür Ü, Alivov YI, Liu C, Teke A, Reshchikov MA, Doğan S, Avrutin V, Cho SJ, Morko¸ H. A comprehensive review of ZnO materials and devices. Journal of Applied Physics. 2005;**98**:1-103. DOI: 10.1063/1.1992666

[34] Janotti A, Van de Walle CG. Fundamentals of zinc oxide as a semiconductor. Reports on Progress in Physics. 2009;**72**:126501. DOI: 10.1088/0034-4885/72/12/126501

[35] Janotti A, Van de Walle CG. Hydrogen multicentre bonds. Nature Materials. 2007;**6**:44-47. DOI: 10.1038/nmat1795

[36] Brox-Nilsen C, Jin J, Luo Y, Bao P, Song AM. Sputtered ZnO thin-film transistors with carrier mobility over 50 $cm^2 V^{-1} s^{-1}$. IEEE Transcations on Electron Devices. 2013;**60**:3424-3429. DOI: 10.1109/TED.2013.2279401

[37] Kim H, Gilmore CM, Piqué A, Horwitz JS, Mattoussi H, Murata H, Kafafi ZH, Chrisey DB. Electrical, optical, and structural properties of indium–tin–oxide thin films for organic light-emitting devices. Journal of Applied Physics. 1999;**86**:6451. DOI: 10.1063/1.371708

[38] Kamiya T, Nomura K, Hosono H. Present status of amorphous In–Ga–Zn–O thin-film transistors. Science and Technology of Advanced Materials. 2010;**11**:44305

[39] Lin Y-Y, Hsu C-C, Tseng M-H, Shyue J-J, Tsai F-Y. Stable and high-performance flexible ZnO thin-film transistors by atomic layer deposition. ACS Applied Materials & Interfaces. 2015;**7**:22610-22617. DOI: 10.1021/acsami.5b07278

[40] Cui Q, Chandra S, McCahan S. The effect of dissolving gases or solids in water droplets boiling on a hot surface. Journal of Heat Transfer. 2001;**123**:719. DOI: 10.1115/1.1376394

[41] Schroder DK. Semiconductor Material and Device Characterization. Hoboken, NJ, USA: John Wiley & Sons, Inc.; 2005. 599 p. DOI: 10.1002/0471749095

[42] Sze SM, Ng KK. Physics of Semiconductor Devices. Hoboken, NJ, USA: John Wiley & Sons, Inc.; 2006. 815 p. DOI: 10.1002/0470068329

[43] Varma T, Periasamy C, Boolchandani D. Performance evaluation of bottom gate ZnO based thin film transistors with different W/L ratios for UV sensing. Superlattices and Microstructures. 2018;**114**:284-295. DOI: 10.1016/j.spmi.2017.12.054

[44] Vidor FF, Meyers T, Hilleringmann U, Wirth GI. Influence of UV irradiation and humidity on a low-cost ZnO nanoparticle TFT for flexible electronics. IEEE-NANO 2015-15th International Conference on Nanotechnology, Vol. 2. 2015. pp. 1179-1181. DOI: 10.1109/NANO.2015.7388836

[45] Jin Y, Wang J, Sun B, Blakesley JC, Greenham NC. Solution-processed ultraviolet photodetectors based on colloidal ZnO nanoparticles. Nano Letters. 2008;**8**:1649-1653. DOI: 10.1021/nl0803702

IntechOpen